Advances and Applications in Mathematical Sciences
Volume 18, Issue 10, August 2019, Pages 1039-1053

MULTIGRID SOLUTION TO ANALYZE THE EFFECT OF ROUGHNESS FOR MODIFIED REYNOLDS EQUATION

SHALINI M. PATIL[1,*], P. A. DINESH[2] and C. V. VINAY[1]

[1]JSS Academy of Technical Education
Bangalore-560060, Karnataka, India

[2]Ramaiaha Institute of Technology
Bangalore-560054, Karnataka, India

Abstract

An attempt is made to understand the significance of unevenness amidst dual lateral surfaces. For this physical configuration magnetic field is applied in cross wise direction. The structure describes that the top portion has irregular covering and descending plate is covered by porous material. To avoid friction, taking into account of contribution of couple-stress fluid is highlighted in this work. The governing equation for this configuration is resolved by desirable boundary conditions. The phenomenal modified Reynolds equation is resolved by adopting one of the leading techniques finite difference based multigrid method. As a result the roughness parameter is discussed relative to numerous values of couple-stress limitations, Hartmann number and aspect ratio to analyze bearing attributes like pressure dissemination and weight bearing capacity. The results and conclusions are summarized with various graphs.

1. Introduction

Several industries are following the magneto hydrodynamic (MHD) lubrication concept in recent technology. There is a high requirement for liquid metals at really superior temperature. The application of industrial lubricants can be observed in various mechanizations related to turbines, compressors, bearings and hydraulic systems. Several analytical and empirical researches have occurred in the MHD lubrication. Squeeze film lubrication is demanding in modern industries as the magnetic field has much practical utilization. The review of literature about the hydrodynamic lubrication by several scientists and researchers is discussed in this section.

2010 Mathematics Subject Classification: 05C50.
Keywords: couple-stress, Hartmann number, porous, multigrid.
*Corresponding author; E-mail: shahem_blr@yahoo.co.in
Received July 25, 2019; Accepted September 22, 2019

Anwar [1] examined the behavior of smoothly moving bearings in the existence of MHD. The theoretical and practical observation about the behavior of thrust bearing in MHD lubrication under outermost pressure was analyzed by Maki [2].

In the occurrence of magnetic field Kamiyam [3] investigated the behavior of squeeze film bearings. The influence of magnetic field for squeeze film lubrication for centrally located dual rotating surfaces was scrutinized by Hamza [4]. Squeeze film lubrication enclosed by coarse and porous equilateral surfaces was studied by solving MHD Reynolds equation by Kudenatti [5].

The efficiency of bearing attributes just as pressure variation, weight carrying capacity and squeezing time was analyzed by Naduvinamani [6] in continuation with magnetic field. Large numbers of researchers are motivated by this unique character of uneven surfaces. In various types of bearings a step was taken to strengthen the performance of hydrodynamic lubrication. There are various hypotheses to describe the uneven nature; the most popular was given by Christensen [7]. Bujurke [8] adopted stochastic theory and explored the effects of roughness on compressed foil attributes among dual rectilinear surfaces of which the top surface has roughness configuration and lower is covered by porous component.

There are several hypotheses to justify the nature of fluids. Stokes [9] micro-continuum hypothesis enlightens the concept of fluid indicating the transparent conclusion which specifies the polar influences like the behavior of couple stresses, body couples and anti-symmetric stress tensor in a continuous medium. To interpret hydrodynamic lubrication problems several researchers have utilized proposal made by Stokes, to name a few Kudenatti [10], Lin [11] and [12]. Taking into account of couple-stress enclosed by 2 lateral surfaces in continuation with MHD was explored by Shalini [13].

2. Physical Configuration

The schematic depiction of the geometrical composition of this work is exhibited by Figure 1. For this model we consider two rectangular symmetric plates. The top surface is irregular and the lower surface is covered with porous structure. To avoid the friction, wear and tear between the sliding

surfaces the lubricating fluid incorporated is viscous and electrically conducting couple stress fluid. Along transverse z inclination an unvarying field of currents M_0 is imposed. The displacement from upper plate towards lower is given by constant velocity $\frac{dH}{dt}$. The lubricating fluid has film density H which separates the upper and lower plate.

The film density H consists of bilateral sections

$$H = h(t) + h_s(x, y, \xi). \tag{1}$$

The film thickness is composed of two segments; the first part is $h(t)$ serves as the factual flat component of the film geometry, at the same time the next segment $h_s(x, y, \xi)$ denotes the level unevenness calculated against the formal plane and which fluctuates arbitrarily with mean equal to zero. ξ is the indicator resolving a precise roughness structure.

Apart from the interpretations of lubrication theory and also considering the limitations, fluid inertia and body forces are neglected in the presence of Lorentz force. In the above situations the predominant equalizations are

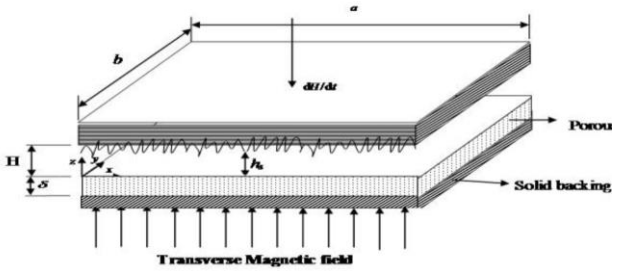

Figure 1. Geometrical representation between coarse and porous surfaces.

$$\frac{\partial u}{\partial x} + \frac{\partial v}{\partial y} + \frac{\partial w}{\partial z} = 0 \tag{2}$$

$$\frac{\partial p}{\partial x} = \mu \frac{\partial^2 u}{\partial z^2} - \eta \frac{\partial^4 u}{\partial z^4} - \sigma M_0^2 u \tag{3}$$

$$\frac{\partial p}{\partial y} = \mu \frac{\partial^2 v}{\partial z^2} - \eta \frac{\partial^4 v}{\partial z^4} - \sigma M_0^2 v \tag{4}$$

$$\frac{\partial p}{\partial z} = 0, \tag{5}$$

where viscosity is μ, couple-stress is η, pressure p, fluid velocity components in x, y and z path are u, v and w, σ is electrical conductivity and magnetic field is M_0.

3. Boundary Situations

The adequate boundary conditions at the upper surface $z = H$,

$$u(x, y, 0) = 0, v(x, y, 0), = 0, w = \frac{\partial H}{\partial t} \tag{6}$$

$$\frac{\partial^2 u}{\partial z^2} = 0, \frac{\partial^2 v}{\partial z^2} = 0. \tag{7}$$

At lower surface $z = 0$

$$\frac{\partial u}{\partial z} = \frac{\alpha}{\sqrt{k}}(u - u^*) \tag{8}$$

$$\frac{\partial v}{\partial z} = \frac{\alpha}{\sqrt{k}}(v - v^*) \tag{9}$$

$$w = w^* \tag{10}$$

$$\frac{\partial^2 u}{\partial z^2} = 0, \frac{\partial^2 v}{\partial z^2} = 0. \tag{11}$$

As a consequence of Beavers and Joseph [14] slip conditions, equations (8) and (9) are considered. The parameter accounts for permeability is k and non-dimensional slip parameter is α.

The below mentioned polar consequences can be observed as a result of modified Darcy's law controlling the flow of fluid in the porous field.

$$\left.\begin{aligned} u^* &= \frac{-k}{\mu(1 - \beta + \phi M^2)} \frac{\partial P^*}{\partial x}, \\ v^* &= \frac{-k}{\mu(1 - \beta + \phi M^2)} \frac{\partial P^*}{\partial y}, \\ w^* &= \frac{-k}{\mu(1 - \beta)} \frac{\partial P^*}{\partial z}, \end{aligned}\right\} \tag{12}$$

$$\nabla \cdot q^* = 0. \tag{13}$$

The Darcy velocity factors u^*, v^*, w^* corresponds towards x, y, z inclinations jointly. k denotes permeability of the porous region. The pressure in porous neighbourhood is P^* and $\beta = \eta/\mu k$. The constant β serves as the fraction of microstructure volume to the pore size. In comparison to the pore size, volume of microstructures is actually small. Porous matrix state is attained when β is infinitesimally small compared to unity. Newtonian case results when β tends to zero.

For Laplace relation (14) the porous domain pressure P^* is satisfied by equation (12).

$$\nabla^2 P^* = 0. \tag{14}$$

Integrating Laplace equation (14) relative to z between $-\delta$ and 0, employing the stable backing marginal condition $\frac{\partial P^*}{\partial z} = 0$ at $z = -\delta$ where δ is the heaviness of the porous region. In comparison with fluid film region, heaviness of the porous domain is deeply narrow, which was suggested by Cameron Morgan approximation. Along with this approximation and applying interface boundary division, and adopting interface frontier condition $p = P^*$ at $z = 0$ equation (14) becomes

$$\frac{\partial P^*}{\partial z}\Big|_{z=0} = -\frac{\delta}{B}\left(\frac{\partial^2 p}{\partial x^2} + \frac{\partial^2 p}{\partial y^2}\right) \tag{15}$$

here $B = (1 - \beta + \phi M^2)$.

4. Solution Procedure

Solution for equation (3) and equation (4) are obtained in terms of u and v by applying the boundary conditions given by equation (6) and equation (11).

$$u = \frac{Q_1 N_1 + Q_2 N_2 + Q_3 N_3 + Q_4 N_4}{Q_5} - \frac{D_1}{\mu D_2}\frac{\partial p}{\partial x}$$

$$v = \frac{Q_{11} N_1 + Q_{22} N_2 + Q_{33} N_3 + Q_{44} N_4}{Q_5} - \frac{D_1}{\mu D_2}\frac{\partial p}{\partial y}$$

where

$$Q_1 = \frac{\alpha D_1 D_4^2}{\sqrt{k}\mu D_2 D_3^3} p_x - \frac{\alpha D_4^2 u^*}{\sqrt{k} D_3^3} - \frac{D_1 D_4^3}{\mu D_2 D_3 (D_3^2 - D_4^2) J_2} p_x$$

$$+ \frac{D_1 D_4^4}{\mu D_2 D_3^2 (D_3^2 - D_4^2) J_1} p_x,$$

$$Q_2 = \frac{\alpha D_1 D_4^2 J_5}{\sqrt{k}\mu D_2 D_3^3} p_x + \frac{\alpha D_4^2 u^* J_5}{\sqrt{k} D_3^3} + \frac{D_1 D_4^3 J_5}{\mu D_2 D_3 (D_3^2 - D_4^2) J_2} p_x$$

$$- \frac{\alpha D_1 D_4^2}{\mu D_2 D_3 (D_3^2 - D_4^2) J_1} p_x + \frac{\alpha D_1 D_4^4}{\sqrt{k}\mu D_2 D_3^3 (D_3^2 - D_4^2) J_1} p_x$$

$$- \frac{D_1 D_4^3 J_6}{\mu D_2 D_3 (D_3^2 - D_4^2) J_2} p_x,$$

$$Q_3 = \frac{\alpha D_1}{\sqrt{k}\mu D_2 D_3} p_x + \frac{\alpha u^*}{\sqrt{k} D_3} + \frac{D_1 D_4 D_3}{\mu D_2 (D_3^2 - D_4^2) J_2} p_x$$

$$- \frac{D_1 D_4^2}{\mu D_2 (D_3^2 - D_4^2) J_2} p_x,$$

$$Q_4 = \frac{\alpha D_1 D_3}{\sqrt{k}\mu D_2 (D_3^2 - D_4^2) J_2} p_x - \frac{\alpha D_1 D_4^2}{\sqrt{k}\mu D_2 D_3 (D_3^2 - D_4^2) J_2} - \frac{D_1 D_4^2 J_5}{\mu D_2 (D_3^2 - D_4^2) J_2} p_x$$

$$- \frac{\alpha D_1 J_6}{\sqrt{k}\mu D_2 D_3} p_x + \frac{\alpha u^* J_6}{\sqrt{k} D_3} + \frac{D_1 D_4^2 J_6 J_5}{\mu D_2 (D_3^2 - D_4^2) J_1} p_x,$$

$$Q_5 = \frac{\alpha}{\sqrt{k} D_3} - \frac{\alpha D_4^2}{\sqrt{k} D_3^3} + \frac{D_4 J_6}{D_3} - \frac{D_4^2 J_5}{D_3^2}.$$

$N_1 = \cosh(D_3 z)$, $N_2 = \sinh(D_3 z)$, $N_3 = \cosh(D_4 z)$, $N_4 = \sinh(D_4 z)$,

$J_1 = \sinh(D_3 H)$, $J_2 = \sinh(D_4 H)$, $J_3 = \cosh(D_3 H)$, $J_4 = \cosh(D_4 H)$,

$J_5 = \coth(D_3 H),$, $J_6 = \coth(D_4 H)$,

$$D_3 = \sqrt{\frac{D_1}{2} + \frac{1}{2}\sqrt{D_1^2 - 4D_2}},$$

$$D_4 = \sqrt{\frac{D_1}{2} - \frac{1}{2}\sqrt{D_1^2 - 4D_2}},\ D_1 = \tau^2,\ D_2 = \frac{M^2\tau^2}{h_0^2},\ M = \sqrt{\frac{\sigma}{\mu}}M_0 h_0.$$

(Replacing p_x by p_y and u^* by v^* in the above expressions for Q_{11}, Q_{22}, Q_{33} and Q_{44} can be obtained.)

Replacing u and v in equation (2) and integrating relating to z over the fluid layer, adopting extreme situation given by equation (12) and equation (15) is represented by equation (16). This equation represents the dissemination of pressure in the fluid region known as modified Reynolds equation (MRE).

$$\frac{\partial}{\partial x}\left\{\left[\chi(H,\ D_3,\ D_4,\ \alpha) - \frac{k\delta}{\mu(1-\beta+\phi M^2)}\right]p_x\right\}$$

$$+\frac{1}{\lambda^2}\frac{\partial}{\partial y}\left\{\left[\chi(H,\ D_3,\ D_4,\ \alpha) - \frac{k\delta}{\mu(1-\beta+\phi M^2)}\right]p_y\right\} = -\left(\frac{M^2\mu}{h_0^3}\right)\frac{\partial H}{\partial t}. \qquad (16)$$

To examine the influence of roughness, it is necessary to consider the stochastic average of Reynolds equation. The expectancy operator $E(\bullet)$ is specified as

$$E(\bullet) = \int_{-\infty}^{\infty} (\bullet) f(h_s) dh_s,$$

where h_s indicates the stochastic variable. The probability density function (pdf) is $f(h_s)$. According to Christensen stochastic hypothesis to examine the roughness nature

$$f(h_s) = \begin{cases} \dfrac{35}{32c^7}(c^2 - h_s^2)^3, & \text{if } -c < h_s < c, \\ 0, & \text{elsewhere.} \end{cases}$$

The irregular film density is represented by c, which is not steady. The above function dissolves at $c = \pm 3\sigma$, where σ acts as standard deviation.

Roughness pattern can be expressed in two frames particularly, longitudinal and transverse.

A. Longitudinal Roughness

For this pattern, the roughness carries limited edges moving in x-orientation

$$\frac{\partial}{\partial x}\left\{\left[E(\chi(H,\ D_3,\ D_4,\ \alpha))-\frac{k\delta M^2}{1-\beta+\phi M^2}\right]\frac{\partial E(p)}{\partial x}\right\}$$

$$+\frac{1}{\lambda^2}\frac{\partial}{\partial y}\left\{\left[\frac{1}{E(1/\chi(H,\ D_3,\ D_4,\ \alpha))}-\frac{k\delta M^2}{1-\beta+\phi M^2}\right]\frac{\partial E(p)}{\partial y}\right\}=-\mu M^2\frac{dh}{dt}. \quad (17)$$

B. Transverse Roughness

For this pattern, the roughness carries limited edges moving in y-orientation

$$\frac{\partial}{\partial x}\left\{\left[\frac{1}{E(1/\chi(H,\ D_3,\ D_4,\ \alpha))}-\frac{k\delta M^2}{1-\beta+\phi M^2}\right]\frac{\partial E(p)}{\partial x}\right\}$$

$$+\frac{1}{\lambda^2}\frac{\partial}{\partial y}\left\{\left[E(\chi(H,\ D_3,\ D_4,\ \alpha))-\frac{k\delta M^2}{1-\beta+\phi M^2}\right]\frac{\partial E(p)}{\partial y}\right\}=-\mu M^2\frac{dh}{dt}. \quad (18)$$

The stochastic average of the Reynolds equation is considered to investigate the influence of roughness.

$$\frac{\partial}{\partial x}\left\{E\left[\chi(H,\ K_3,\ K_4,\ \alpha)-\frac{k\delta}{1-\beta+\phi M^2}\frac{\partial p}{\partial x}\right]\right\}$$

$$+\frac{1}{\lambda^2}\frac{\partial}{\partial y}\left\{E\left[\chi(H,\ K_3,\ K_4,\ \alpha)-\frac{k\delta}{1-\beta+\phi M^2}\frac{\partial p}{\partial y}\right]\right\}=-\frac{\mu M^2}{h_0^3}\frac{\partial E(H)}{\partial t}. \quad (19)$$

The limiting condition for roughness is $E(p)=0,$ as x varying from 0 to a and y varying from 0 to b.

$$E(H)=h \quad (20)$$

a and b represents the dimension of the plate.

Resulting constants support for non-dimensionalization

$$\bar{x}=\frac{x}{a},\ \bar{y}=\frac{y}{b},\ \lambda=\frac{b}{a},\ S=\frac{\alpha}{\sqrt{k}},\ S=\frac{\overline{S}}{h_0},\ \overline{H}=\frac{H}{h_0},$$

$$\tau=\frac{\bar{\tau}}{h_0},\ \psi=\frac{k\delta}{h_0^3},\ p=-\frac{E(p)h_0^3}{\mu a^2\frac{dh}{dt}},\ C=\frac{c}{h_0}, \quad (21)$$

where p represents pressure in the fluid foil, S is the slip constant, ψ permeability constant, τ is the couple-stress parameter.

Substituting equation (21) in equation (19) and removing bars we get

$$\frac{\partial}{\partial x}\left\{\left[E(\chi(H,\ D_3,\ D_4,\ S))-\frac{M^2\psi}{1-\beta+\phi M^2}\right]p_x\right\}$$

$$+\frac{1}{\lambda^2}\frac{\partial}{\partial y}\left\{\left[\frac{1}{E(1/\chi(H,\ D_3,\ D_4,\ S))}-\frac{M^2\psi}{1-\beta+\phi M^2}\right]p_y\right\}=-M^2, \qquad (22)$$

where

$$\chi(H,\ D_3,\ D_4,\ S)=\frac{\begin{array}{r}U_1+U_2+U_3+U_4+U_5+U_6+U_7+U_8+U_9\\+U_{10}+U_{11}+U_{12}\end{array}}{U_{13}+U_{14}}$$

$$U_1=D_3^4D_4^2+D_3^2D_4^4-2D_3^5SJ_1+2D_3^3D_4^2SJ_1,$$

$$U_2=D_3^2(-D_3^2+D_4^2)J_4(D_4^2+(D_3HD_4^2-2D_3S)J_1,$$

$$U_3=2D_3^2D_4^3J_2-2D_4^5SJ_2+D_3^5D_4J_1J_2,$$

$$U_4=D_3D_4^5J_1J_2-HD_3^5D_4SJ_1J_2,$$

$$U_5=2HD_3^3D_4^3SJ_1J_2-HD_3D_4^5SJ_1J_2,$$

$$U_6=-D_4^2J_3(D_3^2(D_3^2+D_4^2)J_4),$$

$$U_7=-(D_3^2-D_4^2)(D_3^2+D_4(HD_3^2-2S)J_2),$$

$$U_8=\frac{M^2D_3^5\alpha^2J_1}{SB}-\frac{M^2D_3^3D_4^2\alpha^2J_1}{SB},$$

$$U_9=D_3^2(-D_3^2+D_4^2)\frac{M^2D_3\alpha^2}{B}J_4J_1-\frac{M^2\alpha^2D_3^3D_4^3J_1}{SB},$$

$$U_{10}=D_3^2(D_3^2+D_4^2)\frac{M^2K_3\alpha^2}{B}J_4J_1-\frac{M^2\alpha^2D_3^3D_4^3J_2}{SB},$$

$$U_{11}=\frac{D_4^5M^2\alpha^2J_2}{SB},$$

$$U_{12} = D_4^2(D_3^2 - D_4^2)\frac{D_4 M^2 \alpha^2}{S(1 - \beta + \phi M^2)} J_3 J_2,$$

$$U_{13} = D_3^5 D_4^2 J_1 J_4 J_2 - D_4^4 D_3^3 J_1 J_4 J_2,$$

$$U_{14} = D_4^3 D_3^2 (D_3^2 - D_4^2) J_3 J_2 + D_3 D_4 (D_3^2 - D_4^2) J_1 J_2,$$

$$E(\chi(H, D_3, D_4, S)) = \frac{35}{32C^7}\int_{-c}^{c} \chi(H, D_3, D_4, S)(C^2 - h_s^2)^3 dh_s,$$

$$E(1/\chi(H, D_3, D_4, S)) = \frac{35}{32C^7}\int_{-c}^{c} \frac{(C^2 - h_s^2)^3}{\chi(H, D_3, D_4, S)} dh_s,$$

and pressure field becomes 0 as x and y varies from 0 to 1.

5. Mathematical Solution

The elliptic structure of MRE equation (22) is genuinely compound to solve practically. Consequently, it is resolved by adopting finite difference based multigrid method (FDBMG). The finite difference approximations for various terms in equation (22).

$$B_0 p_{i+1, j} + B_1 p_{i-1, j} + B_2 p_{i, j+1} + B_3 p_{i, j-1} + B_4 p_{i, j} = -\lambda^2 R_{i, j} \tag{23}$$

$$B_0 = \frac{\lambda^2 \alpha_{i+\frac{1}{2}, j}}{(\Delta x)^2},\ B_1 = \frac{\lambda^2 \alpha_{i-\frac{1}{2}, j}}{(\Delta x)^2} B_2 = \frac{\alpha_{i, \frac{j+1}{2}}}{(\Delta y)^2},\ B_3 = \frac{\alpha_{i, \frac{j-1}{2}}}{(\Delta y)^2}, R_{i, j} = -M^2, \tag{24}$$

and boundary conditions are

$$p_{0, j} = p_{N, j} = p_{i, 0} = p_{i, N} = 0. \tag{25}$$

Multigrid Method

The FDBMG consists of two operators namely restriction and interpolation operators which help us to resolve the MRE. As finite difference method depends on grids, here the count of grids in all paths is 257x257. As a consequence the number of equations and unidentified parameters in the problem are 257x257. The result of the MRE is determined by adopting the FDBMG method. Using this method the pressure allocation for the fluid film

section is measured. In order to avoid large number of errors, Gauss-Seidel iterations technique is used to smoothen these errors. As a result residual is computed. Restriction operator helps in moving from residual to coarser grid level. It is a part of the procedure to attain the coarsest level by exact isolated grid where this mechanism is recapitulated. Now the finer grid level is reached with the help of interpolation operator. As it is an iteration process, it is continued till the initial finest level is obtained.

6. Results and Discussions

A scientific model is established in order to analyze the attributes of lubrication like pressure dissemination, weight bearing capacity, permeability and other criterion by adopting the hypothesis formulated by Stokes. The contribution of couple-stress as a lubricating fluid is powerful for limited values of τ. In this mathematical model to analyse the attributes of bearings FDBMG method is practised.

A. Pressure distribution (PD)

The divergence of pressure along x and y, by maintaining the supplementary constants at $\tau = 15, \lambda = 1.0, H = 0.5, \psi = 0.0001$ and $C = 0.1$, the graphs are plotted by varying $M = 1, 5$ and 7 which is shown by Figures (2-4) respectively. It is convinced from these graphs that the magnetic number M enhances divergence of pressure in this region. The depreciation in lubricant velocity is a consequence of magnetic field perpendicular to the flow. In this fashion enormous volume of fluid is preserved in this segment, as a result pressure distribution enhances.

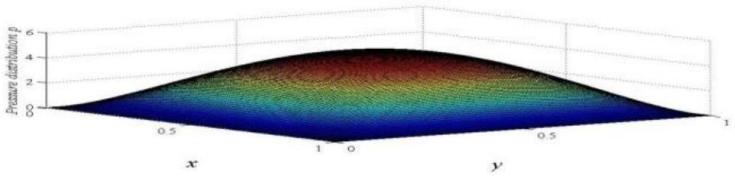

Figure 2. Dissemination of pressure p Vs x and y at $M = 1.0$.

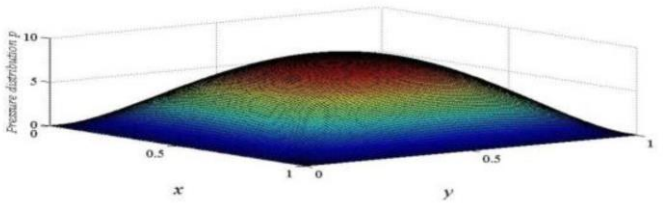

Figure 3. Dissemination of pressure p Vs x and y at $M = 5.0$.

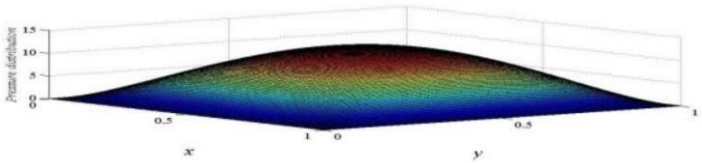

Figure 4. Dissemination of pressure p Vs x and y at $M = 7.0$.

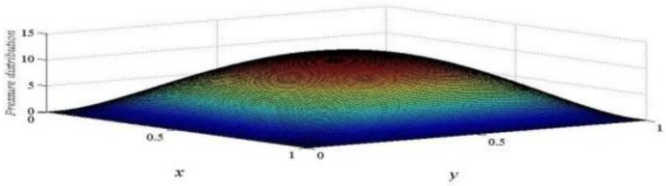

Figure 5. Dissemination of pressure p Vs x and y at $C = 0.1$.

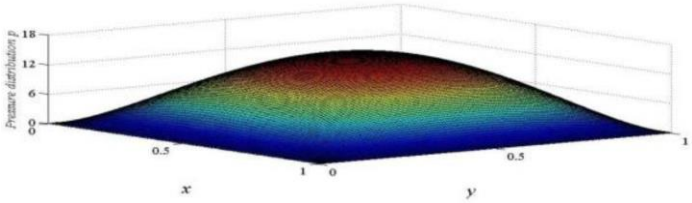

Figure 6. Dissemination of pressure p Vs x and y at $C = 0.3$.

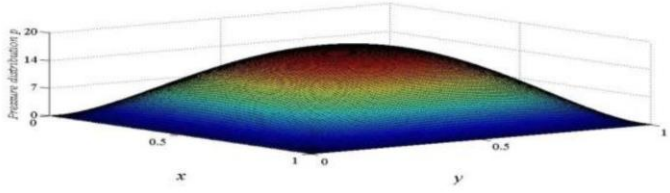

Figure 7. Dissemination of pressure p Vs x and y at $C = 0.4$.

Figures (5-7) exhibit the distribution of pressure corresponding x and y for distinct values of C, maintaining the other variants M, λ, H, ψ and τ as constants. As C enhances from 0.1 to 0.4, the pressure dissemination improves. The fluid velocity declines due to the reality that improvement in roughness enhances the characters of unevenness. This results in reduction of sidewise leakage of the fluid.

B. Weight bearing capacity (WBC)

Another dominant characteristic of lubrication is weight bearing capacity (WBC). This is computed provided previously the fluid film pressure is determined.

$$W = \int_0^1 \int_0^1 p(x, y)dx\,dy$$

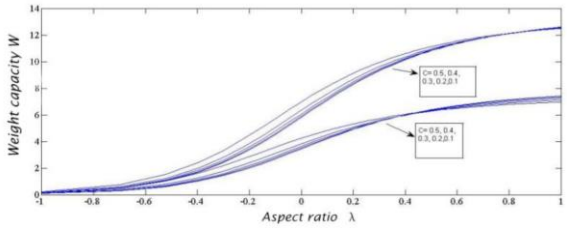

Figure 8. Deviation of WBC W Vs aspect ratio λ.

The interesting point in Figure 8 is for two set of values of roughness C, the distribution of WBC W as a mapping of aspect ratio λ, by maintaining the remaining variables as constants is seen. The appealing remark in the graph assures the critical value of λ where unevenness dissolves. Thus WBC improves as a significance of roughness. Nevertheless, as the aspect ratio enhances from 0.1 to 10, WBC accelerates.

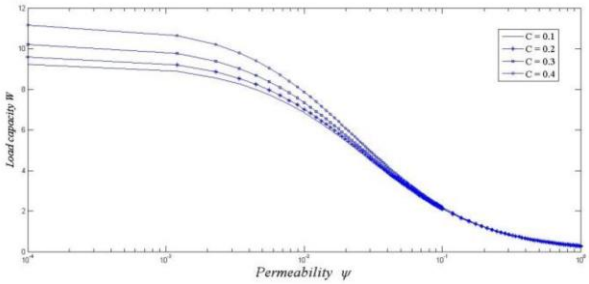

Figure 9. Deviation of WBC W Vs permeability ψ.

Figure 9 interprets the mapping of permeability ψ in contrast to deviation of WBC W for distinct values of C maintaining related variables as constant. It is convinced that WBC improves as C increases. Increase in permeability from 0.0001 to 1.0, is responsible for boosting the WBC. The velocity of the fluid diminishes as an influence of roughness, which contributes for improvement in the PD. Accordingly WBC also enhances.

1. The weight bearing capacity WBC and pressure dissemination (PD) improves as roughness constant C accelerates.

2. The Hartmann number M strengthens the bearing aspects like PD and WBC.

3. Increase in permeability depreciates the bearing aspects like PD and WBC.

4. Also WBC enhances as the aspect ratio λ increases.

References

[1] M. I. Anwar and C. M. Rodkiewicz, Nonuniform magnetic field effects in MHD slider bearings, ASME Journal of Lubrication Technology 94 (1972), 101-105.

[2] E. R. Maki, D. C. Kuzma and R. L. Donnelly, Magnetohydrodynamic lubrication flow between parallel plates, Journal of Fluid Mechanics 26(3) (1966), 537-543.

[3] S. Kamiyama, Magnetohydrodynamic journal bearing (report 1), ASME Journal of Lubrication Technology 91 (1969), 380-386.

[4] E. A. Hamza, The magnetohydrodynamic effects on a fluid film squeezed between two rotating surfaces, Journal of Physics D 24 (1991), 547-554.

[5] R. B. Kudenatti, Shalini M. Patil, P. A. Dinesh and C. V. Vinay, Numerical study of surface porous rectangular plates, Mathematical Problems in Engineering. 2013: pp 1-8.

[6] N. B Naduvinamani, S. T. Fathima and S. Jamal, Effect of roughness on hydromagnetic squeeze films between porous rectangular plates, Tribology International 43(11) (2010), 2145-2151.

[7] H. Christensen, Stochastic model for hydrodynamic lubrication of rough surfaces, Proceedings of Institute of Mechanical Engineering. 1969. Part-I, pp 84:1013.

[8] N. M. Bujurke, N. B Naduvinamani and D. P. Basti, Effect of surface roughness of magnetohydrodynamic squeeze film characteristics between finite rectangular plates, Tribology International 44(7) (2011), 916-921.

[9] V. K. Stokes, Couple stresses in fluids, Physics of Fluids 9 (1966), 1709-1715.

[10] R. B. Kudenatti, D. P. Basti and N. M. Bujurke, Numerical solution of MHD Reynolds

equation for squeeze film lubrication between two parallel surfaces, Applied Mathematics and Computation 218(18) (2012), 9372-9382.

[11] Jaw-Ren-Lin, Magnetohydrodynamic squeeze film characteristics for finite rectangular plates, Industrial Lubrication and Tribology 55(2) (2003), 84-89.

[12] Jaw-Ren-Lin, Rong-Fang Lu and Won-Hsion Liao, Analysis of magnetohydrodynamic squeeze film characteristics between curved annular plates, Industrial Lubrication and Tribology 56(5) (2004), 300-305.

[13] Shalini M. Patil, P. A. Dinesh and C. V. Vinay, Combined effects of couple-stress and MHD on squeeze film lubrication between two parallel plates, International Journal of Mathematical Archive 4(12) (2013), 165-171.

[14] G. S. Beavers and D. D. Joseph, Boundary conditions at a naturally permeable wall, Journal of Fluid Mechanics 30(1) (1967), 197-207.